Mechanism of Taurine: α-Ketoglutarate Dioxygenase (TauD) from *Escherichia coli*

J. Martin Bollinger Jr.,*[a,b] John C. Price,[a] Lee M. Hoffart,[a] Eric W. Barr,[a] and Carsten Krebs*[a,b]

Keywords: Bioinorganic chemistry / Metalloenzymes / Reaction intermediates / Oxygen activation / Iron

The iron(II)- and α-ketoglutarate-dependent dioxygenases comprise enzymes that catalyze a variety of important reactions in biology, including steps in the biosynthesis of collagen and antibiotics, the degradation of xenobiotics, the repair of alkylated DNA, and the sensing of oxygen and response to hypoxia. In these reactions, the reductive activation of oxygen is coupled to hydroxylation of the substrate and decarboxylation of the co-substrate, α-ketoglutarate. It is believed that a single, conserved mechanistic pathway for formation of a high-valent iron intermediate that attacks the substrate is operant in all members of this family. Application of a combination of rapid kinetic and spectroscopic techniques to the reaction of taurine/α-ketoglutarate dioxygenase (TauD), one member of this large enzyme family, has led to the detection of two reaction intermediates. The first intermediate, which is termed **J**, is a high-spin Fe^{IV}-oxo complex. Decay of **J** exhibits a large, normal C1 deuterium kinetic isotope effect, demonstrating that it is the species activating the C–H bond for hydroxylation. The second intermediate is an Fe^{II}-containing product(s) complex.

1. Introduction

The Fe^{II}- and α-ketoglutarate (αKG)-dependent dioxygenases are a large and functionally diverse family of enzymes that employ a structurally conserved, mononuclear, non-heme Fe^{II} center.[1–4] The Fe^{II} center is facially coordinated by three protein ligands, two histidines and one aspartate or glutamate.[5,6] These residues are organized in a His-Xxx-(Asp/Glu)-$(Xxx)_n$-His sequence motif.[3] The Fe^{II} center is used to activate dioxygen to effect (1) the decarboxylation of the co-substrate, αKG, and (2) a two-electron oxidation of the substrate. In most cases the substrate oxidation is a hydroxylation of an unactivated carbon atom, although other two-electron oxidations, such as desaturation and cyclization reactions, are effected by some family members.[3,4]

The αKG-dependent dioxygenases catalyze a wide variety of reactions with diverse biological functions, which have recently been summarized by Hausinger.[3] They catalyze reactions involved in the degradation of xenobiotics,[7] and the biosyntheses of connective tissue,[8,9] various antibiotics,[10–12] and a wide variety of plant secondary metabolites, including flavonoids, gibberellins, and alkaloids (see ref.[3] and references cited therein). In addition, the dysfunction of members of the αKG-dependent dioxygenase family has been implicated in the etiology of several disease states.[13]

Recently, several additional reactions of importance to human biochemistry have been found to be catalyzed by αKG-dependent dioxygenases. The first involves repair of alkylated DNA and RNA by the enzyme AlkB.[14,15] Studies on AlkB from *E. coli* have demonstrated that it can hydroxylate the N-linked carbon of alkyl groups on 1-alkyladenine and 3-alkylcytosine residues in DNA and RNA, leading to elimination of the potentially mutagenic substituent and repair of the base.[14–16] Eight putative homologues of AlkB have been identified in humans, but they are less well studied than *E. coli* AlkB.[14,17]

The second involves control of oxygen homeostasis by the transcription factor, hypoxia inducible factor (HIF).[18,19] When oxygen levels drop, an adaptive response is initiated by the HIF-mediated transcriptional activation of genes that, for example, direct synthesis of new blood vessels (angiogenesis) and production of red blood cells

[a] Department of Biochemistry and Molecular Biology, The Pennsylvania State University,
University Park, PA 16802, USA
Fax: +1-814-863-7024
E-mail: jmb21@psu.edu
ckrebs@psu.edu
[b] Department of Chemistry, The Pennsylvania State University,
University Park, PA 16802, USA

MICROREVIEWS: This feature introduces the readers to the authors' research through a concise overview of the selected topic. Reference to important work from others in the field is included.

(erythropoiesis) to combat hypoxia.[20] HIF activity is controlled by posttranslational hydroxylation of specific amino acid residues in its α-subunit. These reactions are catalyzed by two αKG-dependent dioxygenases. Because molecular oxygen is a co-substrate, the activities of the enzymes provide the mechanism by which oxygen levels are sensed by cells. The first enzyme is the HIF-specific prolyl-4-hydroxylase, which hydroxylates Pro564 of the HIFα-protein.[18,19] Hydroxylated HIFα forms a complex with the von Hippel-Lindau (VHL) tumor suppressor protein, is ubiquitinated, and consequently is subject to proteasomal degradation. The second enzyme catalyzes the hydroxylation of a specific asparagine, Asn803.[21,22] This enzyme has been termed FIH, *f*actor *i*nhibiting *H*IF. Hydroxylation of Asn803 prevents binding of HIFα to the transcriptional coactivator, p300, rendering it (HIFα) inactive. These processes play important roles in the pathophysiology of human diseases, including cancer, cardiovascular, and pulmonary diseases.[20,23] Manipulation of these processes is thus considered a promising strategy for drug design.[24,25]

The third process contributes to iron homeostasis by controlling the activity of the iron regulatory protein 2 (IRP2). It is known that IRP2 is posttranslationally modified, and that modified IRP2 is subject to ubiquitination and proteasomal degradation.[26,27] This process is remarkably similar to the constitutive degradation of the HIFα-protein in oxygen homeostasis. Current evidence suggests that the posttranslational modification of IRP2 is also carried out by a αKG-dependent dioxygenase.[28,29]

2. Mechanism

It is thought that the αKG-dependent dioxygenases use a conserved mechanistic pathway to activate O_2 and form a high-valent iron intermediate that attacks the substrate, leading to hydroxylation or a related two-electron oxidation.[3,4,30] The consensus mechanism for hydroxylation was first formulated by Hanauske-Abel and Günzler solely on the basis of theoretical considerations.[31] Nevertheless, it has thus far held up to the experimental and computational scrutiny of the enzymes and inorganic models of them that has since been carried out. A modified version of this mechanism, adapted for the specific case of the enzyme taurine/αKG dioxygenase (TauD) from *E. coli*, is shown in Scheme 1. The first step in the mechanism is binding of αKG in a chelating mode to the binary enzyme·Fe^{II} complex, a step that gives rise to a weak ($\varepsilon \approx 200\ M^{-1}\,cm^{-1}$) absorption feature in the visible regime (with a peak at 530 nm in TauD). Solomon and co-workers demonstrated for the enzyme clavaminate synthase by a combination of UV/Visible absorption, CD, and MCD spectroscopy and computational studies that this feature arises from a metal-to-ligand charge transfer (MLCT) transition involving the coordinated αKG ligand.[32] The iron site in the ternary enzyme·Fe^{II}·αKG complex is six-coordinate (6C), nearly octahedral, and in the high-spin configuration. The next step in the consensus mechanism is binding of substrate to the ternary enzyme·Fe^{II}·αKG complex.[33] Substrate binds in the vicinity of the Fe^{II} center, but not directly as a ligand, causing changes in the CD and MCD spectra that are indicative of conversion to a five-coordinate (5C) square-pyramidal Fe^{II} site.[32] Hausinger and co-workers have shown that, for TauD, binding of substrate results in a shift of the peak of the MLCT band from 530 nm to 520 nm.[34] Que and co-workers studied the ternary enzyme·Fe^{II}·αKG and quaternary enzyme·Fe^{II}·αKG·substrate complexes of TauD, as well as model complexes for them, by resonance Raman spectroscopy.[35] The bidentate binding mode of the co-sub-

Lee M. Hoffart (left) obtained his Bachelor of Science in Biochemistry, Genetics, and Mathematics in 2003 from Texas A&M University and joined the Department of Biochemistry and Molecular Biology at Penn State as a graduate student in 2003. He continues the work on the α-ketoglutarate dioxygenases under the supervision of Professors Bollinger and Krebs.

Eric W. Barr (second from left) obtained his Bachelor of Science degree in Biochemistry in 1998 from Temple University. He joined Professor Bollinger's group in 2001 as a research assistant and works on the mechanism of oxygen activation by the enzyme taurine/α-ketoglutarate dioxygenase.

John C. Price (middle) obtained his Bachelor of Arts in Chemistry in 2001 from Utah State University, where he worked under the supervision of Professor Lisa Berreau. He joined the Department of Biochemistry and Molecular Biology at Penn State as a graduate student in 2001. His thesis work, which he carries out under the supervision of Professors Bollinger and Krebs, is on the mechanism of oxygen activation by the enzyme taurine/α-ketoglutarate dioxygenase.

Carsten Krebs (second from right) received his Diploma in Chemistry in 1994 and his Ph.D. in Chemistry in 1997 from the Ruhr-University of Bochum, Germany, under the supervision of Professor Karl Wieghardt. In 1997 he joined the group of Professor Boi Hanh (Vincent) Huynh in the Department of Physics at Emory University, Atlanta. In 2002, he joined the Department of Biochemistry and Molecular Biology at the Pennsylvania State University as Assistant Professor. In 2004 he was appointed to the Department of Chemistry at Penn State. His research interest is the determination of the reaction mechanisms of iron-containing enzymes.

J. Martin Bollinger Jr. (right) received his Bachelor of Science degree in Chemistry from Penn State University in 1986 and his Ph.D. degree in Chemistry in 1993 from the Massachusetts Institute of Technology, where he worked under the direction of Professor JoAnne Stubbe. After an N.I.H. post-doctoral fellowship with Professor Christopher Walsh at Harvard Medical School, Professor Bollinger joined the department of Biochemistry and Molecular Biology at Penn State in 1995. He was promoted to Associate Professor in 2002 and appointed to the Department of Chemistry in 2004. His work focuses on enzyme reaction mechanisms, particularly those of iron-dependent oxygenases.

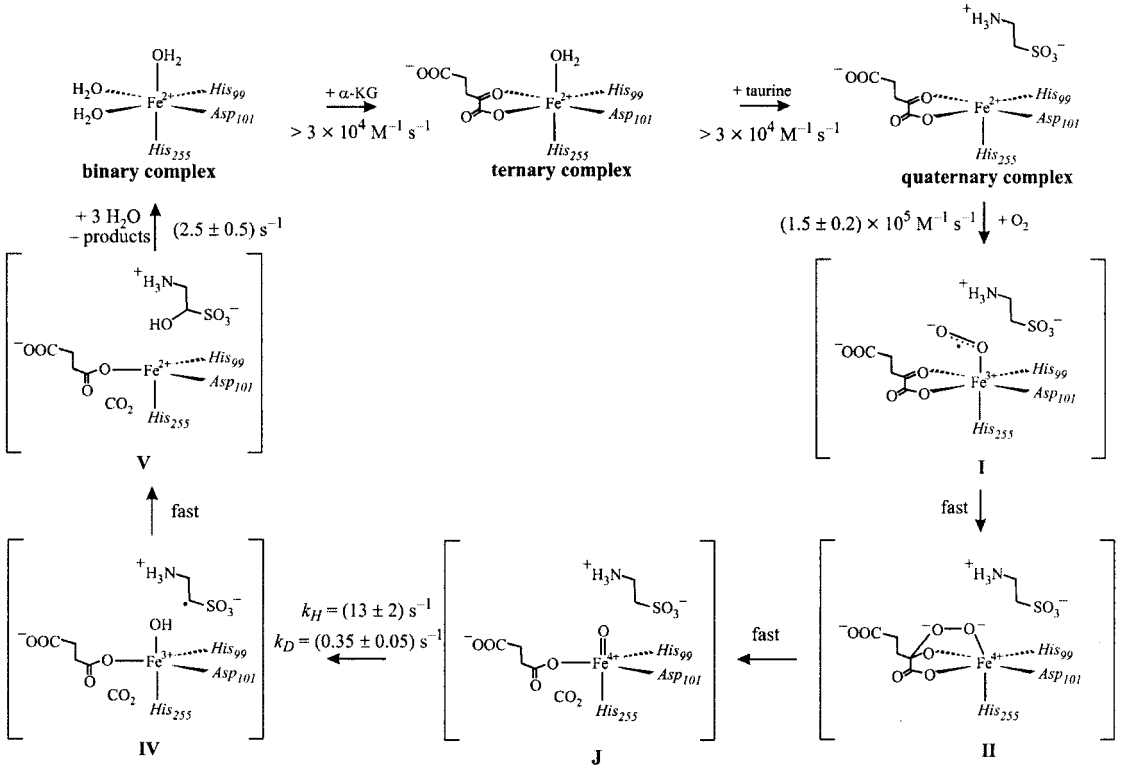

Scheme 1. Consensus mechanism for the Fe^{II}- and α-ketoglutarate-dependent dioxygenases, adapted for the specific case of taurine/α-ketoglutarate dioxygenase. The assignment of rate constants at 5 °C to individual steps of the mechanism is based on refs.[39,61,68,72,78]

strate, αKG, has also been demonstrated by X-ray crystallographic studies of a number of αKG-dependent dioxygenases (see ref.[3] and references cited therein). The structures reveal that the carbonyl group of αKG binds *trans* to the protein carboxylate ligand, whereas the C1 carboxylate group of αKG binds opposite to one of the histidine residues. Interestingly, it can bind either *trans* to the histidine of the His-Xxx-Asp/Glu-motif, which is termed "in line" binding mode, or it can bind *trans* to the histidine more distant in sequence ("off line" binding mode).[3] There is X-ray crystallographic evidence for flexibility of αKG-binding in some of the enzymes. For example, in clavaminate synthase, αKG binds "in line" when the substrate analogue deoxyguanidinoproclavaminate is bound, and it binds "off line" when NO as an analogue of oxygen coordinates to the Fe center of the deoxyguanidinoproclavaminate complex.[36] Another example is the enzyme alkyl sulfatase, for which "in line" coordination of αKG to the Fe^{II} center is observed, whereas "off line" binding is observed when the Fe^{II} is substituted with Na^+.[37] In addition, αKG binding is stabilized by the ionic interaction of its C5 carboxylate group with an arginine or lysine residue.

The dissociation of the water ligand creates an open coordination site, and it is proposed that this is the site to which oxygen adds.[4,30] Indeed, it has been shown that binding of the substrate increases reactivity toward O_2 many-fold.[38,39] Thus, the enzymes have evolved what amounts to a conformational "trigger" for O_2 activation, which serves to favor the formation of reactive intermediates only in the presence of the target substrate, thereby minimizing the potentially inactivating self-oxidation reactions that have been demonstrated to occur in a number of the enzymes when the ternary enzyme·Fe^{II}·αKG complex reacts with O_2 in the absence of substrate.[40–42] Addition of oxygen to the coordinatively unsaturated Fe^{II} center of the quaternary complex yields intermediate **I**, in which the O_2 moiety is proposed to coordinate end-on to the Fe center. **I** is a $\{FeOO\}^8$ complex, and computational studies from the Solomon group suggest that it should be described as a Fe^{III}-superoxo species.[43] These calculations were calibrated by correlating experimental and computational data for the related $\{FeNO\}^7$ complexes,[43] which have been prepared by addition of NO to the Fe^{II} forms of a number of different mononuclear non-heme enzymes[44,45] and models thereof.[46,47] The postulated Fe^{III}-superoxo complex **I** is proposed to react by a nucleophilic attack of the uncoordinated O atom on C2 of αKG, thereby forming the bicyclic species, **II**. The next step in the proposed mechanism is decarboxylation of αKG and cleavage of the O–O bond to yield an Fe^{IV}-oxo, intermediate, **J**.[48] Alternative structures for the Fe^{IV}-oxo intermediate have been proposed. These include a mixed anhydride of carbonic and succinic acids, in which the O atom is inserted into the C1–C2 bond of αKG.[3] The products of decarboxylation of αKG are succinate and CO_2. Importantly, the mechanism predicts that one O atom of succinate should derive from O_2, and this has been verified for several of the enzymes by use of $^{18}O_2$ (see ref.[3] and references cited therein). In the next step, the Fe^{IV}-oxo intermediate is proposed to abstract a H atom from the substrate, yielding **IV**, which consists of a Fe^{III}–

OH complex and a substrate radical. Although **IV** has never been detected directly, evidence for the formation of a substrate radical was obtained by Begley and co-workers in their study of prolyl-4-hydroxylase (P4H) from *Paramecium bursaria Chlorella virus* 1.[49] P4H-directed oxidation of a peptide substrate containing 5-oxaproline was shown to result in conversion of the proline analogue to aspartate in a process that is likely to involve rearrangement of the expected substrate radical intermediate. In the normal catalytic processes, "oxygen rebound" of the Fe^{III}–OH complex of **IV** with the substrate radical generates the hydroxylated product and a Fe^{II} center. Thus, the mechanism also predicts that the O atom incorporated into the substrate should be derived from dioxygen, and this has also been verified by isotopic labeling experiments. Importantly, incorporation of ^{18}O from O_2 has been shown for some enzymes to be less than stoichiometric, suggesting that the O atom in **J** or **IV** (or both) may exchange with solvent (see ref.[3] and references cited therein). Alternatively, the oxo group may be protonated and a coordinated hydroxide ligand may become deprotonated and be incorporated into the product. This mechanism was named "ferryl-flip".[3] The hydroxide ligand required for this mechanism is not shown in Scheme 1, but coordination of a hydroxide ligand in addition to the ligands shown is entirely possible, especially considering that **J** and **IV** are depicted as having only five ligands.

Significant insight into the mechanism was also obtained from studies on inorganic model complexes.[4] Fe^{IV}-oxo complexes have been synthesized and characterized spectroscopically,[50–54] and oxygen activation by Fe^{II} centers coordinated by α-ketoacids has been investigated in detail.[35,55–59] These studies revealed that the α-ketoacid can bind as a monodentate or bindentate ligand, but only the latter exhibits the diagnostic MLCT band. Decarboxylation is accelerated by electron-withdrawing substituents on the α-ketoacid, consistent with the proposed nucleophilic attack of the superoxo species of **I** on the α-ketone carbonyl.[57]

Although the aforementioned studies provided support for the consensus mechanism, until very recently none of the proposed intermediates (enclosed in brackets in Scheme 1) had been directly detected for any enzyme in the family. In 2002, we selected one member of this enzyme family, TauD, which catalyzes hydroxylation of C1 of taurine (2-aminoethane-1-sulfonic acid) and other organosulfonates to initiate elimination of sulfite for sulfur acquisition,[60] for kinetic studies designed finally to reveal intermediates in this important reaction cycle. Several characteristics made it an ideal choice for such studies.[34] It is relatively small (32 kDa), soluble to high concentration, thermally stable, and readily obtained in large quantity by overexpression in *E. coli*.[34] In addition, its substrate, taurine, is chemically simple, making analogues with chemical or isotopic substitutions designed to perturb the reaction kinetics or mechanism synthetically accessible.

Investigation of the TauD reaction by rapid kinetic (stopped-flow and freeze-quench) and spectroscopic methods (UV/Visible, Mössbauer, EPR, resonance Raman, X-ray absorption) led to the detection of two intermediates in the catalytic cycle not previously detected for any member of the family. These studies are summarized in the following sections.

3. Detection of Two Intermediates in the TauD Reaction

The first evidence for the accumulation of two intermediates was obtained from stopped-flow absorption experiments.[61] Changes in the spectrum after mixing of the quaternary TauD·Fe^{II}·αKG·taurine complex with an oxygenated buffer solution (but not after a control mix with O_2-free buffer) were shown to be dominated by a positive feature at 318 nm, which reaches maximum intensity after approximately 20 ms (Figure 1, A), and a negative feature associated with loss of the chromophoric reactant complex, which develops fully only after the 318 nm feature has decayed (inset to Figure 1, A). These observations were rationalized by a minimal kinetic mechanism involving two accumulating intermediate states, the 318-nm absorbing first intermediate, **J**, which also absorbs into the visible regime to partially compensate for the loss of the absorption from the reactant complex, and a second species lacking both UV and visible absorption that accumulates prior to regeneration of the reactant complex. Rate constants of 1.5×10^5 M^{-1} s^{-1} for formation of **J**, 13 s^{-1} for decay of **J** to the second intermediate, and 2.5 s^{-1} for conversion of this intermediate back to the reactant quaternary complex were shown to accommodate the data well. Kinetic traces at 318 nm and 520 nm illustrate the three-step sequence clearly (Figure 1, B).

Although revealing their accumulation, the stopped-flow absorption experiments provided no clues as to the structures of the two intermediates, nor their positions within the catalytic cycle. Rapid freeze-quench (RFQ) Mössbauer spectroscopy provided the first such clues.[61] Mixing of the quaternary complex, which has a spectrum typical of a high-spin Fe^{II} species (Figure 1, C, top), with O_2-containing buffer results in a new Mössbauer absorption line at +0.75 mm/s (Figure 1, C). With increasing reaction time, the new peak was found to decay (Figure 1, D, filled circles) with the same time-dependence predicted for **J** (Figure 1, D, solid line), thereby establishing that the Mössbauer absorption at +0.75 mm/s is associated with **J**. Analysis of the experimental spectra revealed that **J** exhibits a quadrupole doublet (solid line shown above the spectrum of the 20-ms sample in Figure 1, D) with unusual parameters, an isomer shift (δ) of 0.31 mm/s and a quadrupole splitting parameter (ΔE_Q) of 0.88 mm/s. In general, the reduced isomer shift of **J** suggested that it is an oxidized species, but the value did not allow assignment of oxidation state, because it is higher than any of the isomer shifts reported for Fe^{IV} complexes[51,62–66] but also at the low extreme for high-spin Fe^{III}. Indeed, a trigonal bipyramidal high-spin Fe^{III} model complex reported by MacBeth et al. has the same isomer

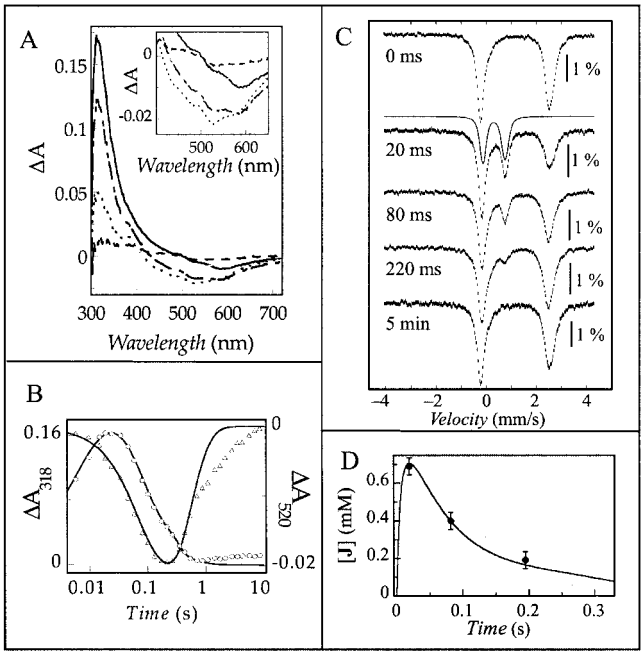

Figure 1. (**A**) UV/Visible absorption spectroscopic changes recorded 20 ms (solid lines), 68 ms (dot-dashed lines), 210 ms (dotted lines), and 10 s (dashed lines) after equal-volume mixing at 5 °C of a solution of 2.4 mM TauD, 2.2 mM Fe^{II}, 10 mM αKG, and 10 mM taurine with O_2-saturated buffer. The inset is a magnification of the absorbance changes in the 500-nm region. (**B**) Absorbance kinetic traces at 318 nm (circles) and 520 nm (triangles). The solid lines are simulations according to the rate constants shown in Scheme 1. (**C**) 4.2-K/40-mT Mössbauer spectra of RFQ samples from the reaction of the TauD·Fe^{II}·αKG·taurine complex with O_2. The reaction times are shown. A simulation of the spectrum of **J** (δ = 0.31 mm/s, ΔE_Q = 0.88 mm/s) is shown as solid line. (**D**) Concentration of **J** determined from RFQ Mössbauer spectroscopy (circles) and a simulation according to Scheme 1 (solid line). All figures are adapted from Price et al.[61]

shift, 0.31 mm/s.[67] Exposure of samples containing high levels of **J** to γ-irradiation at 77 K (cryoreduction) monitored by EPR and Mössbauer spectroscopy was shown to convert it to one (or more) high-spin Fe^{III} complex, establishing the formal oxidation state of **J** as +IV.[61]

Decay of **J** is accompanied by an increase of the intensity of the high-energy line (at ≈ 2.7 mm/s) of the Mössbauer quadrupole doublet of the high-spin Fe^{II} species, demonstrating that the second intermediate contains Fe^{II}.[39]

4. Placement of the Intermediates within the Catalytic Cycle and Integration of the Kinetic and Chemical Mechanisms

The stopped-flow absorption and freeze-quench Mössbauer data by themselves established neither the identities nor the positions within the catalytic cycle of the two intermediates. The formal +IV oxidation state of **J** and +II state of the second intermediate suggested that the former occurs before taurine hydroxylation and the latter after, but the lack of good precedents for intermediates in the catalytic cycle precluded more definitive assignment by simple comparison of Mössbauer and optical properties. For example, it is possible to depict both **I** and **II** (in addition to **J**) with "resonance structures" having the Fe in the +IV oxidation state. Similarly, the second intermediate might be either a product(s) complex or the TauD·Fe^{II} binary complex awaiting rebinding of substrates. Additional kinetic experiments resolved these issues.

4.1 J is the Hydroxylating Intermediate

The position of **J** in the catalytic cycle was resolved by testing for substrate deuterium kinetic isotope effects (KIEs) on formation and decay of the intermediate. 1,1-$[^2H]_2$-taurine and the (control) unlabeled substrate were synthesized and used to prepare the reactant quaternary complex for reaction with O_2. A large normal KIE ($k_H/k_D \approx 37$) on decay of **J**, but no KIE on its formation, were observed. This result was shown both by stopped-flow absorption measurements (Figure 2, A) and by RFQ Mössbauer (Figure 2, B).[68] The result suggests that **J** is responsible for cleavage of the C1-$[^{1,2}H]$ bond, making the most likely identity of the complex the Fe^{IV}-oxo species in Scheme 1. This conclusion was subsequently confirmed by resonance Raman and X-ray absorption spectroscopic experiments (see below).

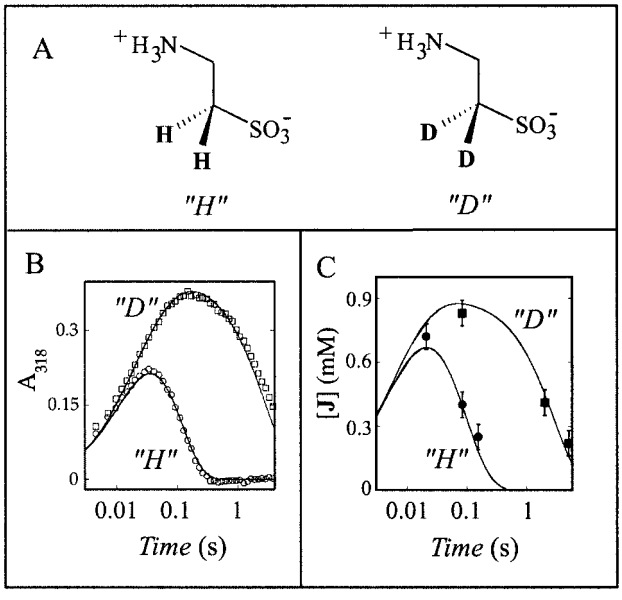

Figure 2. (**A**) Structures of 1,1-$[^1H]_2$-taurine and 1,1-$[^2H]_2$-taurine. Kinetics of **J** monitored by (**B**) stopped-flow absorption and (**C**) RFQ Mössbauer spectroscopy. The circles and squares represent the experimental data obtained using 1,1-$[^1H]_2$-taurine and 1,1-$[^2H]_2$-taurine, respectively. The solid lines are simulations for **J** according to the rate constants shown in Scheme 1. In **B**, a solution containing 2.0 mM TauD, 1.8 mM Fe^{II}, 17 mM αKG and 17 mM taurine was mixed with air-saturated buffer in a volume ratio of 2:5 at 5 °C. In **C**, a solution containing 4 mM TauD, 3.6 mM $^{57}Fe^{II}$, 10 mM αKG, and 10 mM taurine was mixed with an equal volume of O_2-saturated buffer at 5 °C. Adapted from Price et al.[68]

4.2 An Integrated Kinetic/Chemical Mechanism: Verification of its Predictions

The identity of **J** and the apparent failure of precursors to accumulate suggested that **J** forms rapidly after the initial slower addition of O_2 to the quaternary complex. The demonstration of a first-order dependence of the kinetics of formation of **J** on the concentration of O_2 proved this point[69] and allowed an upper limit to be established for the quantity of a precursor that can accumulate.[39] The demonstration by chemical quenched-flow experiments that loss of CO_2 from αKG correlates with formation of **J** established a second important prediction of the integrated mechanism and provided support for the structure assigned to **J**. The large C1 deuterium KIE on conversion of **J** to an Fe^{II} complex, again apparently without accumulation of intervening intermediates (e.g., **IV** in Scheme 1), indicates that the postulated "radical rebound" to the C1 radical is rapid compared to the preceding H atom abstraction. The implication that decay of **J** should be kinetically correlated with formation of product has been verified by chemical quenched-flow experiments quantifying sulfite released by the immediate product, 1-hydroxytaurine. All that remained was to establish the nature of the second intermediate and define the steps involved in its rate-limiting conversion back to the reactant quaternary complex.

4.3 Assignment of the Second Intermediate as a Product Complex

The initial transient-kinetic study on TauD had reported that binding of αKG to the TauD·Fe^{II} binary complex is relatively slow (2–6 s^{-1} at 4 °C) and, somewhat surprisingly for an association reaction, of kinetic order zero in αKG.[34] This report implicated a unimolecular step associated with formation of the TauD·Fe^{II}·αKG complex as the rate-limiting step and suggested that the second intermediate might be the binary complex. Resolution of the Mössbauer spectrum of the second intermediate showed that it is distinct from that of the TauD·Fe^{II} complex and also different from those of the TauD·Fe^{II}·αKG and TauD·Fe^{II}·αKG·taurine complexes.[39] Re-examination of αKG binding by stopped-flow absorption experiments monitoring development of the MLCT band at 530 nm showed that formation of the complex is remarkably complex, but much faster overall than the rate-limiting conversion of the second intermediate back to the reactant complex (Figure 3, A).[39] Taurine binding to the TauD·Fe^{II}·αKG complex is fast, but prior binding of taurine impedes binding of αKG (Figure 3, B), consistent with the preferred or obligatory order of substrate binding that has been seen in the reactions of other members of this family and providing a rationale for inhibition by taurine of both steady-state turnover and quaternary complex re-formation. The demonstration that formation of **J** upon mixing of TauD·Fe^{II} simultaneously with all three substrates is only slightly slower than upon mixing of the quaternary complex with O_2 (and much faster than the 2.5 ± 0.5 s^{-1} decay of the second intermediate) ruled out the possibility that steps involved in substrate binding contribute to the rate-limiting conversion of the second intermediate to the quaternary complex. This conclusion left only steps involved in product dissociation as candidates for the rate-limiting step and implied that the second intermediate is a product(s) complex. Support for these inferences came from examining the dependence of k_{cat} on solvent viscosity. With 1,1-[^{1}H]$_2$-taurine, the significant reduction of k_{cat} by increasing viscosity is consistent with rate-limiting diffusion of product from the active site. By contrast, with 1,1-[^{2}H]$_2$-taurine as substrate, the large KIE renders H atom abstraction rate-limiting, leading to a much less pronounced solvent-viscosity effect.[39]

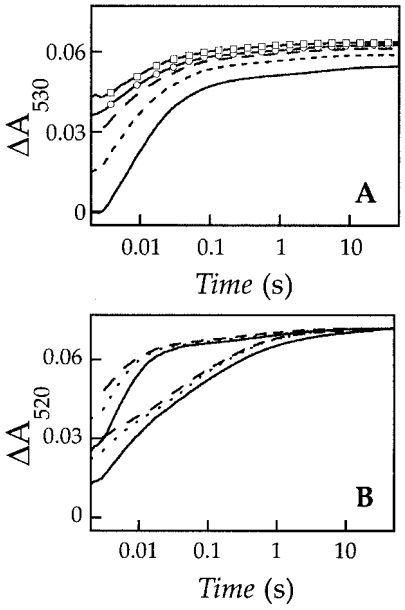

Figure 3. Absorbance-vs.-time traces monitoring binding of αKG in the absence (**A**) and presence (**B**) of taurine. In **A**, TauD containing 0.69 equivalents of Fe^{II} was mixed at 5 °C in the absence of O_2 with solutions of αKG to give final concentrations of 0.49 mM TauD and 1.5 mM (solid trace), 3 mM (dotted trace), 6 mM (dashed trace), 9 mM (solid trace with open circles), or 15 mM (solid trace with open squares) αKG. In **B**, both sets of traces are from experiments in which TauD containing 0.69 equivalents of Fe^{II} was mixed with a solution of αKG to give final concentrations of 0.49 mM TauD and 3 mM (solid traces), 6 mM (dotted traces), or 9 mM (dashed traces) αKG. For the lower three traces, taurine was present in the TauD·Fe^{II} solution such that [taurine] was 5 mM after mixing. In the upper three traces, taurine was present in the αKG solution, also giving 5 mM taurine after mixing. Adapted from Price et al.[39]

5. Structural Characterization of J

The results described in Sections 3 and 4 established that **J** contains a (formally) Fe^{IV} center and that it cleaves the C1–H bond of taurine to initiate its hydroxylation. In the consensus mechanism, the C1–H abstracting species is an Fe^{IV}-oxo species. Characterization of **J** by a variety of spectroscopic and computational methods described in the following sections demonstrated that **J** is indeed the long-pos-

tulated Fe^{IV}-oxo complex. Interestingly, the Fe center of **J** is in the high-spin ($S = 2$) configuration.

5.1 Mössbauer Spectroscopy

Mössbauer spectra of **J** recorded in varying external magnetic fields allowed for the determination of the spin state of the Fe center and the associated zero-field splitting (ZFS) parameters, D and E/D. The facts that **J** gives rise to a quadrupole doublet in a weak (40-mT) magnetic field but displays increasing magnetic splitting with increasing externally applied magnetic field is typical of paramagnetic complexes with (almost) axial integer-spin electronic ground states and $D > 0$. The 8-T spectrum of **J** exhibits six sharp lines with peak separations that reflect an effective magnetic field of about 24 T experienced by the ^{57}Fe nucleus, corresponding to an internal magnetic field of ca. 32 T oriented antiparallel to the externally applied 8-T field (Figure 4, A).[61] The magnitude of the internal magnetic field is much larger than those experimentally observed for the many low-spin ($S = 1$) heme and non-heme Fe^{IV}-oxo compounds,[50–52,62,70] suggesting that S of the Fe^{IV} site in **J** is larger than 1. To illustrate this point, a simulation of the spectrum of a low-spin ($S = 1$) non-heme Fe^{IV}-oxo complex is shown in part B of Figure 4 for comparison.[51] Analysis of the field-dependent spectra under the assumption that the Fe^{IV} site of **J** is in the high-spin ($S = 2$) configuration yielded $D = 10.5\ cm^{-1}$, $E/D = 0.03$, $g = (2.0, 2.0, 2.0)$ (fixed), $\delta = 0.31$ mm/s, $\Delta E_Q = -0.88$ mm/s, $\eta = 0$ (fixed), and $A/g_N\beta_N = (-18\ T, -18\ T,$ not determined).[71] Interestingly, these parameters are similar to those observed for the high-spin Fe^{IV} site of intermediate **X** from *E. coli* ribonucleotide reductase,[65] thereby corroborating the assignment of **J** as a high-spin Fe^{IV} species.

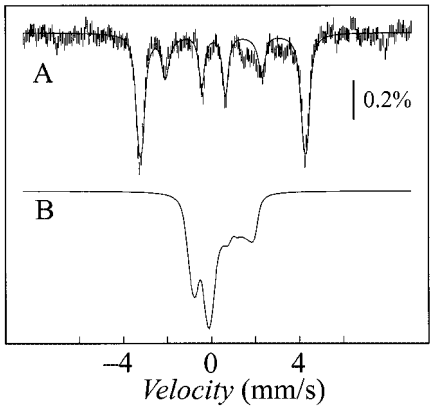

Figure 4. (**A**) 4.2-K/8-T Mössbauer reference spectrum of **J**. The solid line is a spin Hamiltonian simulation according to parameters given in the text. (**B**) Theoretical simulation of the spectrum of the low-spin Fe^{IV}-oxo complex reported by Rohde et al.: $S = 1$, $D = 29\ cm^{-1}$, $E/D = 0$, $g = (2.3, 2.3, 2.0)$, $\delta = 0.17$ mm/s, $\Delta E_Q = 1.24$ mm/s, $\eta = 0.5$, $A/g_N\beta_N = (-22.5, -18.2, -2.9)$ T.[51]

5.2 Resonance Raman Spectroscopy

The assignment of **J** as an Fe^{IV}-oxo complex was to this point based solely on chemical precedent and intuition. Resonance Raman experiments by Proshlyakov et al. provided the first direct evidence for the assignment.[72] One of the spectroscopic hallmarks of the Fe^{IV}-oxo unit is a vibrational frequency in the 800 cm^{-1} region which is downshifted by approximately 35 cm^{-1} for the ^{18}O isotopomer.[73] This downshift is close to the value predicted for a Fe–O diatomic harmonic oscillator. Proshlyakov et al.[72] succeeded in obtaining the stretching frequency of the Fe^{IV}-oxo unit of **J** by using continuous flow of reactants (quaternary complex and O_2) at low temperature (- 38 °C) to generate the intermediate and collecting at a distance from the mixer corresponding to a reaction time of 150 ms. This time was selected on the basis of absorption data recorded under the same experimental conditions, which suggested that the concentration of **J** would be at its maximum then. Resonance Raman difference spectra, which were obtained from the reaction carried out with either $^{16}O_2$ or $^{18}O_2$, revealed bands at 821 cm^{-1} ($^{16}O_2$) and 789 cm^{-1} ($^{18}O_2$). The energies of these bands are close to those observed in resonance Raman spectra of Fe^{IV}-oxo units found in heme enzymes and heme and non-heme model complexes.[51,73] Consequently, these features were attributed to the Fe=O stretching frequency.

In addition to the vibration of the Fe^{IV}-oxo unit, the authors observed a second O isotope-sensitive feature at 583 cm^{-1} ($^{16}O_2$) and 555 cm^{-1} ($^{18}O_2$). Because Fe^{IV}-oxo species do not exhibit a band in this region, the authors reasoned that it originates from a different intermediate. Interestingly, terminally coordinated Fe^{III}-superoxo oxyhemoglobins exhibit the Fe–O stretching frequency in this region, in addition to the O–O stretching frequency in the 1130 cm^{-1} region.[74] The authors did indeed observe a derivative band in the 1100 to 1160 cm^{-1} spectral region, but it overlaps with an intense solvent band, hence not allowing for its unambiguous assignment. This raises the possibility that the features at 583 (555) cm^{-1} may also emanate from a Fe^{III}-superoxo species, e.g. structure **I** of Scheme 1. Whereas this assignment is plausible, the vast quantities of protein required and the inflexibility of the apparatus necessitated by the extraordinary technical demands of the experiment prevented the crucial demonstration of the expected time-dependent decrease in the ratio of intensities of the 583/555 cm^{-1} band of the putative precursor and the 821/789 cm^{-1} band of **J**. If the lower energy feature does indeed arise from a precursor to **J**, the complex should be detectable by RFQ Mössbauer experiments carried out with similar reaction conditions, because it should have an integer-spin ground state, give rise to a quadrupole doublet at 4.2 K in a small externally applied magnetic field, and, therefore, be detectable even at relatively modest concentrations.

5.3 X-ray Absorption Spectroscopy

The second prominent characteristic of the Fe^{IV}-oxo group is a short (ca. 1.65 Å) Fe–O bond.[51,52,70,75–77] Because of the high reactivity of the Fe^{IV}-oxo unit, the bond

length generally cannot be determined using X-ray crystallography. The recent report of the first X-ray structure of a Fe^{IV}-oxo non-heme model complex is a remarkable exception.[51] For the case of **J**, the Fe–O distance was determined by X-ray absorption spectroscopy.[78] These experiments required that the Fe^{IV}-oxo complex be the predominant species in the sample. Accumulation of **J** to 80% of the Fe in the sample was made possible by the use of 1,1-$[^2H]_2$-taurine and the large deuterium KIE on decay of **J**.[68] X-ray absorption spectra of samples containing primarily **J** were shown to exhibit the hallmarks of a Fe^{IV}-oxo unit. First, the edge energy is significantly higher than that of the quaternary TauD·Fe^{II}·αKG·taurine complex, suggesting that **J** is in a high oxidation state. Second, the pre-edge feature caused by the 1s→3d transitions is intense, which is caused by the less centrosymmetric ligand environment of the Fe center imposed by the oxo ligand. Third, fitting of the EXAFS region of the spectra requires the assumption of a short, 1.62 Å, interaction between the Fe and one of its ligands. Importantly, the coordination number for this short interaction was found to range from 0.5 to 0.8, in agreement with the fraction of **J** in the sample determined independently by Mössbauer spectroscopy. On the basis of the extensive precedent, the 1.62 Å interaction was assigned to the Fe^{IV}-oxo unit.

5.4 Proposed Structure of J

The data indicate that **J** has an Fe^{IV}-oxo unit with the iron in high-spin configuration. To the best of our knowledge, the only other example of a high-spin Fe^{IV}-oxo unit is a dinuclear model complex.[79] Importantly, the large number of characterized mononuclear heme and non-heme Fe^{IV}-oxo species all have a low-spin (S = 1) Fe^{IV}-oxo group.[50–52,62,70] In a trigonal bipyramidal ligand field the d-orbitals split into two low-lying *e*-sets and one orbital high in energy (d_{z^2}). To evaluate the possibility that the four low-lying orbitals can accommodate four unpaired electrons, resulting in the experimentally observed S = 2 configuration, density functional calculations on the trigonal bipyramidal model of **J** shown in Figure 5 were conducted.[71] This model contains two imidazole ligands (one axial and one equatorial), two equatorial carboxylate ligands, and the axial oxo ligand. The three protein ligands derived from the $(His)_2$-$(Asp)_1$ triad are represented by the two imidazole ligands and one of the carboxylate ligands. They coordinate the Fe center facially. The second equatorial carboxylate ligand mimics one of the products of the reaction, succinate. The other product of the decarboxylation reaction, CO_2, has not been included in this model, although interactions of CO_2 with the Fe center have been reported. Coordination of CO_2, derived from hydrogencarbonate in the buffer, to the Fe^{II} center opposite to the more distant (in sequence) histidine has been detected by X-ray crystallography for deacetoxycephalosporin C synthase,[80] and by perturbation of the Fe^{III}-catecholate chromophore in TauD, which is obtained by the self-hydroxylation of tyrosine 73 followed by coordination of the catecholate to the iron.[40] Geometry optimization of the model of **J** does not result in significant structural changes and yields a lower energy for the S = 2 state, suggesting that the trigonal bipyramidal geometry is one way of rationalizing the high-spin state of the Fe^{IV} center of **J**.

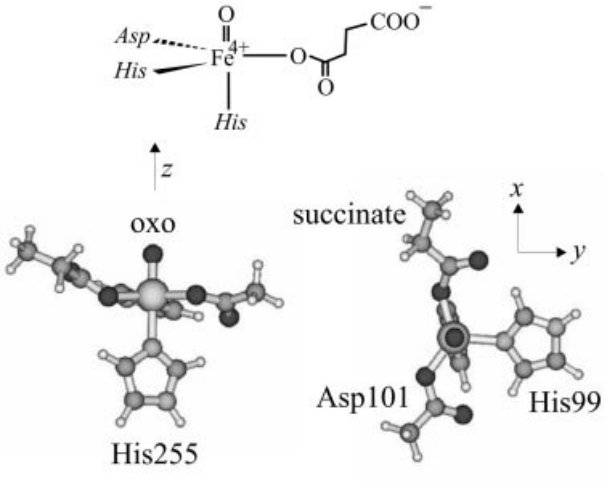

Figure 5. Structural model of intermediate **J** in TauD obtained by DFT calculations. Adapted from Krebs et al.[71]

As noted, the Mössbauer isomer shift of **J** is unusually high, approaching values observed for high-spin Fe^{III} complexes.[67] Because DFT methods can predict Mössbauer parameters with considerable accuracy,[81–84] the comparison of calculated and experimental parameters provides a means of validating structural models for reactive intermediates of unknown structure. Although the Mössbauer isomer shift of the trigonal bipyramidal model calculated by this approach (0.22 mm/s) is lower than the experimentally observed isomer shift of **J** (0.31 mm/s), the deviation is still within the uncertainty of the method (0.10 mm/s).[81] Although further calculations, in particular those taking into account the effect of the protein, are clearly warranted to more rigorously evaluate potential structures for **J**, the agreement between theory and experiment suggests that **J** may have a trigonal bipyramidal structure with an axial oxo ligand.

6. Conclusion and Outlook

Two intermediates detected in the reaction of the quaternary TauD·Fe^{II}·αKG·taurine complex with oxygen have been assigned by a combination of rapid kinetic and spectroscopic methods as a high-spin Fe^{IV}-oxo species, **J**, which abstracts H from C1 of taurine, and a product(s) complex, **V** in Scheme 1, that releases product in the rate-limiting step of the catalytic cycle. Other intermediates in the consensus mechanism are kinetically masked, and therefore do not accumulate. Current efforts are directed towards accumulation of these intermediate states for their spectroscopic characterization. For example, the resonance Raman spectroscopic studies by Proshlyakov et al. suggest that in-

termediate **I** or **II** may accumulate when the reaction is carried out at low temperature (–35 °C).[72] Perturbation of the reaction kinetics by the use of substrate analogues, variant proteins, or both may also allow for accumulation and characterization of additional complexes in the cycle.

Acknowledgments

We thank our collaborators and co-workers, whose work is reported in this article. This work has been supported by the Pennsylvania State University (startup funds to C. K.) and grant from the National Institutes of Health (NIH-GM 69657 to J. M. B. and C. K.).

[1] R. Y. N. Ho, L. Que Jr., *Chem. Rev.* **1996**, *96*, 2607–2624.
[2] M. J. Ryle, R. P. Hausinger, *Curr. Opin. Chem. Biol.* **2002**, *6*, 193–201.
[3] R. P. Hausinger, *Crit. Rev. Biochem. Mol. Biol.* **2004**, *39*, 21–68.
[4] M. Costas, M. P. Mehn, M. P. Jensen, L. Que Jr., *Chem. Rev.* **2004**, *104*, 939–986.
[5] L. Que Jr., *Nature Struct. Biol.* **2000**, *7*, 182–184.
[6] K. D. Koehntop, J. P. Emerson, L. Que Jr., *J. Biol. Inorg. Chem.* **2005**, *10*, 87–93.
[7] R. P. Hausinger, F. Fukumori, D. A. Hogan, T. M. Sassanella, Y. Kamagata, H. Takami, R. E. Saari, in: *Microbial Diversity and Genetics of Biodegradation* (Eds.: K. Horikoshi, M. Fukuda, T. Kudo,); Japan Scientific Press: Tokyo, **1997**, pp. 35–51.
[8] J. J. Hutton Jr., A. L. Tappel, S. Udenfriend, *Biochem. Biophys. Res. Commun.* **1966**, *24*, 179–184.
[9] K. I. Kivirikko, T. Pihlajaniemi, *Adv. Enzymol. Rel. Areas Mol. Biol.* **1998**, *72*, 325–398.
[10] M. D. Lloyd, K. D. Merritt, V. Lee, T. J. Sewell, B. Wha-Son, J. E. Baldwin, C. J. Schofield, S. W. Elson, K. H. Baggaley, N. H. Nicholson, *Tetrahedron* **1999**, *55*, 10201–10220.
[11] R. W. Busby, M. D. T. Chang, R. C. Busby, J. Wimp, C. A. Townsend, *J. Biol. Chem.* **1995**, *270*, 4262–4269.
[12] J. E. Baldwin, R. M. Adlington, J. B. Coates, M. J. C. Crabbe, N. P. Crouch, J. W. Keeping, G. C. Knight, C. J. Schofield, H. H. Ting, C. A. Vallejo, M. Thorniley, E. P. Abraham, *Biochem. J.* **1987**, *245*, 831–841.
[13] A. G. Prescott, M. D. Lloyd, *Nat. Prod. Rep.* **2000**, *17*, 367–383.
[14] T. Duncan, S. C. Trewick, P. Koivisto, P. A. Bates, T. Lindahl, B. Sedgwick, *Proc. Natl. Acad. Sci. U. S. A.* **2002**, *99*, 16660–16665.
[15] S. C. Trewick, T. F. Henshaw, R. P. Hausinger, T. Lindahl, B. Sedgwick, *Nature* **2002**, *419*, 174–178.
[16] P. A. Aas, M. Otterlei, P. O. Falnes, C. B. Vagbo, F. Skorpen, M. Akbari, O. Sundheim, M. Bjoras, G. Slupphaug, E. Seeberg, H. E. Krokan, *Nature* **2003**, *421*, 859–863.
[17] M. A. Kurowski, A. S. Bhagwat, G. Papaj, J. M. Bujnicki, *BMC Genomics* **2003**, *4*, 48.
[18] M. Ivan, K. Kondo, H. Yang, W. Kim, J. Valiando, M. Ohh, A. Salic, J. M. Asara, W. S. Lane, W. G. Kaelin Jr., *Science* **2001**, *292*, 464–468.
[19] P. Jaakkola, D. R. Mol, Y.-M. Tian, M. I. Wilson, J. Gielbert, S. J. Gaskell, A. von Kriegsheim, H. F. Hebestreit, M. Mukherji, C. J. Schofield, P. H. Maxwell, C. W. Pugh, P. J. Ratcliffe, *Science* **2001**, *292*, 468–472.
[20] C. J. Schofield, P. J. Ratcliffe, *Nat. Rev. Mol. Cell Biol.* **2004**, *5*, 343–354.
[21] K. S. Hewitson, L. A. McNeill, M. V. Riordan, Y.-M. Tian, A. N. Bullock, R. W. Welford, J. M. Elkins, N. J. Oldham, S. Bhattacharya, J. M. Gleadle, P. J. Ratcliffe, C. W. Pugh, C. J. Schofield, *J. Biol. Chem.* **2002**, *277*, 26351–26355.
[22] P. C. Mahon, K. Hirota, G. L. Semenza, *Genes Dev.* **2001**, *15*, 2675–2686.
[23] G. L. Semenza, *Nature Rev. Cancer* **2003**, *3*, 721–732.
[24] K. S. Hewitson, C. J. Schofield, *Drug Discovery Today* **2004**, *9*, 704–711.
[25] K. S. Hewitson, L. A. McNeill, C. J. Schofield, *Curr. Pharm. Des.* **2004**, *10*, 821–833.
[26] K. Iwai, R. D. Klausner, T. A. Rouault, *EMBO J.* **1995**, *14*, 5350–5357.
[27] K. Iwai, S. K. Drake, N. B. Wehr, A. M. Weissman, T. Lavaute, N. Minato, R. D. Klausner, R. L. Levine, T. A. Rouault, *Proc. Natl. Acad. Sci. U. S. A.* **1998**, *95*, 4924–4928.
[28] E. S. Hanson, M. L. Rawlins, E. A. Leibold, *J. Biol. Chem.* **2003**, *278*, 40337–40342.
[29] J. Wang, G. Chen, M. Muckenthaler, B. Galy, M. W. Hentze, K. Pantopoulos, *Mol. Cell. Biol.* **2004**, *24*, 954–965.
[30] E. I. Solomon, T. C. Brunold, M. I. Davis, J. N. Kemsley, S.-K. Lee, N. Lehnert, F. Neese, A. J. Skulan, Y.-S. Yang, J. Zhou, *Chem. Rev.* **2000**, *100*, 235–349.
[31] H. M. Hanauske-Abel, V. Günzler, *J. Theor. Biol.* **1982**, *94*, 421–455.
[32] E. G. Pavel, J. Zhou, R. W. Busby, M. Gunsior, C. A. Townsend, E. I. Solomon, *J. Am. Chem. Soc.* **1998**, *120*, 743–753.
[33] In contrast, for the enzyme prolyl-4-hydroxylase, it was reported that binding of oxygen occurs prior to binding of substrate (R. Myllylä, L. Tuderman, K. I. Kivirikko, *Eur. J. Biochem.* **1977**, *80*, 349–357; M. Rundgren, *J. Biol. Chem.* **1977**, *252*, 5094–5099).
[34] M. J. Ryle, R. Padmakumar, R. P. Hausinger, *Biochemistry* **1999**, *38*, 15278–15286.
[35] R. Y. N. Ho, M. P. Mehn, E. L. Hegg, A. Liu, M. J. Ryle, R. P. Hausinger, L. Que Jr., *J. Am. Chem. Soc.* **2001**, *123*, 5022–5029.
[36] Z. Zhang, J.-s. Ren, K. Harlos, C. H. McKinnon, I. J. Clifton, C. J. Schofield, *FEBS Lett.* **2002**, *517*, 7–12.
[37] I. Müller, A. Kahnert, T. Pape, G. M. Sheldrick, W. Meyer-Klaucke, T. Dierks, M. Kertesz, I. Usón, *Biochemistry* **2004**, *43*, 3075–3088.
[38] M. J. Ryle, A. Liu, R. B. Muthukumaran, R. Y. N. Ho, K. D. Koehntop, J. McCracken, L. Que Jr., R. P. Hausinger, *Biochemistry* **2003**, *42*, 1854–1862.
[39] J. C. Price, E. W. Barr, L. M. Hoffart, C. Krebs, J. M. Bollinger Jr., *Biochemistry* **2005**, *44*, 8138–8147.
[40] M. J. Ryle, K. D. Koehntop, A. Liu, L. Que Jr., R. P. Hausinger, *Proc. Natl. Acad. Sci. U. S. A.* **2003**, *100*, 3790–3795.
[41] A. Liu, R. Y. N. Ho, L. Que Jr., M. J. Ryle, B. S. Phinney, R. P. Hausinger, *J. Am. Chem. Soc.* **2001**, *123*, 5126–5127.
[42] T. F. Henshaw, M. Feig, R. P. Hausinger, *J. Inorg. Biochem.* **2004**, *98*, 856–861.
[43] G. Schenk, M. Y. M. Pau, E. I. Solomon, *J. Am. Chem. Soc.* **2004**, *126*, 505–515.
[44] D. M. Arciero, A. M. Orville, J. D. Lipscomb, *J. Biol. Chem.* **1985**, *260*, 14035–14044.
[45] V. J. Chen, A. M. Orville, M. R. Harpel, C. A. Frolik, K. K. Surerus, E. Münck, J. D. Lipscomb, *J. Biol. Chem.* **1989**, *264*, 21677–21681.
[46] K. Pohl, K. Wieghardt, B. Nuber, J. Weiss, *J. Chem. Soc. Dalton Trans.* **1987**, 187–192.
[47] M. Ray, A. P. Golombek, M. P. Hendrich, G. P. A. Yap, L. M. Liable-Sands, A. L. Rheingold, A. S. Borovik, *Inorg. Chem.* **1999**, *38*, 3110–3115.
[48] Footnote, We called the Fe^{IV}-oxo complex previously **III**. Results obtained by us and others allowed assignment of the intermediate **J** to this structure.
[49] M. Wu, H.-S. Moon, T. P. Begley, J. Myllyharju, K. I. Kivirikko, *J. Am. Chem. Soc.* **1999**, *121*, 587–588.
[50] C. A. Grapperhaus, B. Mienert, E. Bill, T. Weyhermüller, K. Wieghardt, *Inorg. Chem.* **2000**, *39*, 5306–5317.
[51] J.-U. Rohde, J.-H. In, M. H. Lim, W. W. Brennessel, M. R. Bukowski, A. Stubna, E. Münck, W. Nam, L. Que Jr., *Science* **2003**, *299*, 1037–1039.

[52] M. H. Lim, J.-U. Rohde, A. Stubna, M. R. Bukowski, M. Costas, R. Y. N. Ho, E. Münck, W. Nam, L. Que Jr., *Proc. Natl. Acad. Sci. U. S. A.* **2003**, *100*, 3665–3670.
[53] J. Kaizer, M. Costas, L. Que Jr., *Angew. Chem. Int. Ed.* **2003**, *42*, 3671–3673.
[54] A. Decker, J.-U. Rohde, L. Que Jr., E. I. Solomon, *J. Am. Chem. Soc.* **2004**, *126*, 5378–5379.
[55] E. H. Ha, R. Y. N. Ho, J. F. Kisiel, J. S. Valentine, *Inorg. Chem.* **1995**, *34*, 2265–2266.
[56] Y.-M. Chiou, L. Que Jr., *J. Am. Chem. Soc.* **1995**, *117*, 3999–4013.
[57] M. P. Mehn, K. Fujisawa, E. L. Hegg, L. Que Jr., *J. Am. Chem. Soc.* **2003**, *125*, 7828–7842.
[58] S. Hikichi, T. Ogihara, K. Fujisawa, N. Kitajima, M. Akita, Y. Moro-oka, *Inorg. Chem.* **1997**, *36*, 4539–4547.
[59] Y.-M. Chiou, L. Que Jr., *Inorg. Chem.* **1995**, *34*, 3577–3578.
[60] E. Eichhorn, J. R. van der Ploeg, M. A. Kertesz, T. Leisinger, *J. Biol. Chem.* **1997**, *272*, 23031–23036.
[61] J. C. Price, E. W. Barr, B. Tirupati, J. M. Bollinger Jr., C. Krebs, *Biochemistry* **2003**, *42*, 7497–7508.
[62] P. G. Debrunner, *Phys. Bioinorg. Chem. Ser.* **1989**, *4*, 137–234.
[63] S. K. Lee, B. G. Fox, W. A. Froland, J. D. Lipscomb, E. Münck, *J. Am. Chem. Soc.* **1993**, *115*, 6450–6451.
[64] K. E. Liu, D. Wang, B. H. Huynh, D. E. Edmondson, A. Salifoglou, S. J. Lippard, *J. Am. Chem. Soc.* **1994**, *116*, 7465–7466.
[65] B. E. Sturgeon, D. Burdi, S. Chen, B. H. Huynh, D. E. Edmondson, J. Stubbe, B. M. Hoffman, *J. Am. Chem. Soc.* **1996**, *118*, 7551–7557.
[66] D. Lee, B. Pierce, C. Krebs, M. P. Hendrich, B. H. Huynh, S. J. Lippard, *J. Am. Chem. Soc.* **2002**, *124*, 3993–4007.
[67] C. E. MacBeth, A. P. Golombek, V. G. Young Jr., C. Yang, K. Kuczera, M. P. Hendrich, A. S. Borovik, *Science* **2000**, *289*, 938–941.
[68] J. C. Price, E. W. Barr, T. E. Glass, C. Krebs, J. M. Bollinger Jr., *J. Am. Chem. Soc.* **2003**, *125*, 13008–13009.
[69] P. K. Grzyska, M. J. Ryle, G. R. Monterosso, J. Liu, D. P. Ballou, R. P. Hausinger, *Biochemistry* **2005**, *44*, 3845–3855.
[70] T. Wolter, W. Meyer-Klaucke, M. Müther, D. Mandon, H. Winkler, A. X. Trautwein, R. Weiss, *J. Inorg. Biochem.* **2000**, *78*, 117–122.
[71] C. Krebs, J. C. Price, J. Baldwin, L. Saleh, M. T. Green, J. M. Bollinger Jr., *Inorg. Chem.* **2005**, *44*, 742–757.
[72] D. A. Proshlyakov, T. F. Henshaw, G. R. Monterosso, M. J. Ryle, R. P. Hausinger, *J. Am. Chem. Soc.* **2004**, *126*, 1022–1023.
[73] T. Kitagawa, Y. Mizutani, *Coord. Chem. Rev.* **1994**, *135/136*, 685–735.
[74] T. K. Das, M. Couture, Y. Ouellet, M. Guertin, D. L. Rousseau, *Proc. Natl. Acad. Sci. U. S. A.* **2001**, *98*, 479–484.
[75] M. Chance, L. Powers, T. Poulos, B. Chance, *Biochemistry* **1986**, *25*, 1266–1270.
[76] J. E. Penner-Hahn, K. Smith Eble, T. J. McMurry, M. Renner, A. L. Balch, J. T. Groves, J. H. Dawson, K. O. Hodgson, *J. Am. Chem. Soc.* **1986**, *108*, 7819–7825.
[77] J.-U. Rohde, S. Torelli, X. Shan, M. H. Lim, E. J. Klinker, J. Kaizer, K. Chen, W. Nam, L. Que Jr., *J. Am. Chem. Soc.* **2004**, *126*, 16750–16761.
[78] P. J. Riggs-Gelasco, J. C. Price, R. B. Guyer, J. H. Brehm, E. W. Barr, J. M. Bollinger Jr., C. Krebs, *J. Am. Chem. Soc.* **2004**, *126*, 8108–8109.
[79] H. Zheng, S. J. Yoo, E. Münck, L. Que Jr., *J. Am. Chem. Soc.* **2000**, *122*, 3789–3790.
[80] H.-J. Lee, M. D. Lloyd, K. Harlos, I. J. Clifton, J. E. Baldwin, C. J. Schofield, *J. Mol. Biol.* **2001**, *308*, 937–948.
[81] F. Neese, *Inorg. Chim. Acta* **2002**, *337*, 181–192.
[82] F. Neese, *Curr. Opin. Chem. Biol.* **2003**, *7*, 125–135.
[83] Y. Zhang, J. Mao, N. Godbout, E. Oldfield, *J. Am. Chem. Soc.* **2002**, *124*, 13921–13930.
[84] V. Vrajmasu, E. Münck, E. L. Bominaar, *Inorg. Chem.* **2003**, *42*, 5974–5988.

Received: May 25, 2005
Published Online: September 16, 2005

